ENVIRONMENTAL ENGINEERING SCIENCE
Volume 14, Number 3, 1997
Mary Ann Liebert, Inc.

Treatment of Acid-Mine Water with Calcite and Quartz Sand

CHARLIE Y. XU,[1] FRANKLIN W. SCHWARTZ,[2] and SAMUEL J. TRAINA[3]

[1]*Department of Earth and Environmental Sciences*
University of Illinois
Chicago, IL 60607-7059
[2]*Department of Geological Sciences*
[3]*School of Natural Resources*
The Ohio State University
Columbus, OH 43210

ABSTRACT

This study investigates interactions between a typical acid-mine water and a solid mixture of calcite and quartz. In this solid mixture, calcite provides a source of alkalinity whereas quartz surfaces become preferable place for precipitation of produced oxides. The results indicate that neutralization by calcite dissolution is critical for extensive immobilization of metals from these waters. As pH increases, ferrihydrite, amorphous $Al(OH)_3$, $Cu(OH)_2$, and possibly $Zn(OH)_2$ precipitate that decreases the aqueous concentrations of Fe, Al, Cu, and Zn. These precipitates also provide more adsorption sites for metal ions. Under the experimental conditions used in this study, Pb sorption was stronger than either Cd or Zn. The presence of ferrihydrite increased Pb and Cd adsorption significantly. Cd was most mobile with respect to the other metal ions studied. Besides metal ions, SO_4^{2-} is also adsorbed onto oxide surfaces to some extent. An unknown sulfate mineral was present when the mine water lacked dissolved Fe or was not neutralized by calcite. The mineral is likely a Cu and/or Zn sulfate with structural H_2O.

Key words: Acid mine; treatment; quartz; calcite

INTRODUCTION

ACID-MINE DRAINAGE (AMD) RESULTS FROM the weathering of sulfide minerals, such as pyrite (FeS_2) and its polymorph marcasite (α-FeS) by exposure to oxygenated surface water or groundwater (Faure, 1991). Acid-mine waters typically exhibit low pH values with relatively large concentrations of dissolved sulfate and Fe and potentially toxic concentrations of heavy metals (e.g., Pb, As). Transport of heavy metals to streams, lakes, and groundwater aquifers may lead to a significant degradation in water quality.

Three important types of reactions operate to control the concentrations of metals and sulfur in AMD: oxidation/reduction (redox), dissolution/precipitation, and surface adsorption reactions. Accelerated oxidation of ferrous Fe by the bacteria *Thiobacillus ferrooxidans* (Omura et al., 1991; Bigham et al., 1990; 1992) favors the precipitation of iron oxides, oxyhydroxides, and oxyhydroxysulfates, resulting in the co-precipitation of metals such as As and Se (Omura et al., 1991; Bigham et al., 1991, 1992; Merrill et al., 1986). Biological reduction forces metal sulfide precipitation under reducing conditions which often exist in natural or constructed wetlands (Machemer and Wildeman, 1992; Chironis, 1929).

Precipitation of dissolved iron also can be achieved electrochemically (Jenke and Diebold, 1984), or by raising the solution pH with lime or other substitutes (Boling et al., 1992; Heunis, 1987; Bates et al., 1990). Metal adsorption to the surfaces of various Fe and Al oxides, hydroxides, and oxyhydroxides may also act to reduce metal concentrations in solution. Of the possible solids,

ferrihydrite, a poorly crystalline Fe hydroxide (nominally $Fe_5HO_8 \cdot 4H_2O$) is one of the most important because of its abundance and its high surface area and reactivity (Dzombak and Morel, 1990).

The objective of this study is to examine the process of metal immobilization as acid-mine waters react with a mixture of calcite and quartz sand. An improved understanding of the interactions between contaminants in acid-mine waters and the solid mixture can assist in the design of reactive control systems to treat water AMD.

MATERIALS AND METHODS

The acid-mine water used in the experiments was synthetically prepared in the laboratory according to a recipe that was based on average compositions of acid-mine waters from coal and metal mines reported in literature (Jenke and Diebold, 1984; Winland, 1989; Winland et al., 1991; Sasowsky and White, 1993; Hammen et al., 1993; Filipek et al., 1987). The composition of the synthetic acid-mine water used in this study is given in Table 1. The water composition was verified analytically by Inductively Coupled Plasma (ICP) emission (see Table 1). Preliminary tests showed that precipitation of a yellow solid occurred when the acid water of the composition shown in Table 1 was allowed to age for 10 hours. The solid was identified as ferrihydrite by X-ray diffraction analysis. The minor precipitation of ferrihydrite was probably due to the presence of high SO_4 concentration that was found to accelerate the precipitation even at low pH values (Flynn, 1984). Therefore, samples were prepared less than 30 minutes before each experimental treatment to avoid solid precipitation.

TABLE 1. COMPOSITION OF THE SYNTHETIC ACID-MINE WATER USED IN THE STUDY

Component	*Prepared conc. mg/L*
SO_4^{2-}	960
Cl^-	327
ClO_4^-	2985
NO_3^-	260
Mg^{2+}	24.3
K^+	7.8
Na^+	460
Al^{3+}	27.0
Fe^{3+}	560
Cu^{2+}	127
Cd^{2+}	5.62
Zn^{2+}	131
Pb^{2+}	10.3
pH (measured)	2.42–2.51[a]

[a]The pH range reflects the measurements of the synthetic solution prepared at different times.

The synthetic acid-mine waters were then reacted with Ottawa quartz (α-SiO_2) (Grade 2.6, U.S. Silica Co., Ottawa, IL) and Iceland calcite ($CaCO_3$) (Earth Science Educator's Supply, Lee's Summit, MO). Both quartz and calcite were confirmed by X-ray powder diffraction (XRD) analyses. The quartz sand was sieved and the 60–80 mesh fraction was used in the study. The quartz sand was washed with 1% HCl and rinsed with distilled water to remove carbonates and surface contaminants. The calcite was ground and sieved and the 60–80 mesh fraction was used. The solid samples were reacted in batch with the synthetic acid-mine solutions employing three treatments: (1) quartz sand with no calcite, (2) calcite with no quartz sand, and (3) a mixture of 95% quartz sand and 5% calcite. In some treatments, the synthetic solution not containing Fe^{3+} [as $Fe(ClO_4)_3$] or Pb, Cu, Zn, and Cd (in nitrates) was used to help elucidate the important role of iron and other chemical variations in the reaction system.

Batches of 150 mL solutions were prepared in 250 mL polyethelene plastic bottles according to the initial conditions outlined in Table 2. Experimental procedures are shown schematically in Fig. 1. After thorough mixing of initial solutions, a 4-mL aliquot was pipetted from each bottle for pH measurement. The pH measurement was conducted in a 5-mL Teflon vial containing a Teflon-coated magnet-stirring bar. Nineteen grams of quartz sand and/or 1.0 gram of calcite were added to the remaining (146 mL) solution in each bottle (Table 2). The bottles were sealed with parafilm which was perforated to prevent CO_2 pressure buildup by allowing for exchange with the atmosphere.

The bottles were placed in an Eberbach reciprocal shaker (Ann Arbor, MI) and were shaken for approximately 15 hours at 180 rpm at 25 ± 2°C. After shaking, about 45 mL of suspension from each bottle was transferred to a 50 mL polycarbonate centrifuge tube. The tube was then centrifuged at 1500 rpm for 1 hour and 30 mL of its clear supernatant was decanted as the final solution (Table 2) to a polycarbonate sample bottle. Four mL of the supernatant was pipetted for pH measurement. The remaining supernatant was acidified by adding two drops of 37% HCl and was refrigerated for 2 days before analysis.

The remaining suspension in each bottle was separated from the coarse-grain solids settled on the bottom of the bottle and was transferred to a 50 mL centrifuge tube. The suspended solids were washed repeatedly by centrifuging and decanting supernatant until the suspension became dispersed with fine particles even after cen-

TABLE 2. INITIAL CONDITIONS OF ALL EXPERIMENTAL TREATMENTS

Treatment	*Solution*	*Solid(s)*
11	Composition[a] less Fe	1 g calcite + 19 g quartz
12	Whole composition	1 g calcite + 19 g quartz
13	Composition less Pb, Cu, Zn, Cd	1 g calcite + 19 g quartz
14	Whole composition	Only 1 g calcite
15	Whole composition	Only 19 g quartz

[a]Composition listed in Table 1.

trifuging. About 5 mL of suspension were pipetted onto a glass microscope slide (labeled as SR samples). The remaining suspension in the tube was quickly frozen in a freezer and freeze dried under vacuum. These solids were labeled as CX samples. The coarse-grain solids in the bottles (mainly quartz and calcite) were dried in an oven at 60°C prior to being transferred to 20 mL glass vials for further examinations (R samples).

Sample Analyses

The total Ca, Zn, Cd, Cu, Pb, and Fe concentrations in the acidified supernatant from the experiments were measured with atomic absorption (AA) spectrometry using a Perkin-Elmer 3030B instrument with an air-acetylene flame. Besides these metals, concentrations of Al, K, Mg, Na, and SO_4 were analyzed with an inductively coupled plasma emission spectroscopy (ICP).

Both the SR and CX samples were examined with an X-ray diffractometer (Philips Electronic) using CuKα radiation at 35 kV and 20 mA. The diffraction was digitally reduced in the 2θ range of 10°–70° with 0.05° interval and 4-second count for each 2θ angle for most of the samples. The diffraction peaks obtained from the samples were used for mineral identification with reference to the data files from the Joint Commission of Powder Diffractometry Society (JCPDS). The SR samples also were examined by infrared spectroscopy. A 5-mg sample was mixed with 195 mg of spectroscopic-grade KBr and ground with a sapphire mortar and pestle. The resulting powder was hand-packed into a 3 mm conical sample cup and the upper surface was smoothed with a glass microscope slide. Diffuse reflectance, Fourier Transform Infrared Spectra (DR-FTIR) were obtained for the samples using a Mattson-Polaris FTIR equipped with a broad-band MCT detector. All spectra were recorded as an average of 100 scans made at 2 cm^{-1} resolution in 4000–400 cm^{-1} range.

The CX and R samples were examined with a scanning electron microscope (SEM) using a JEOL JSM-A20 instrument equipped with an energy dispersive X-ray analyzer (EDS). The samples for the SEM analyses were mounted on stainless-steel stubs using double-stick tapes and were coated with gold.

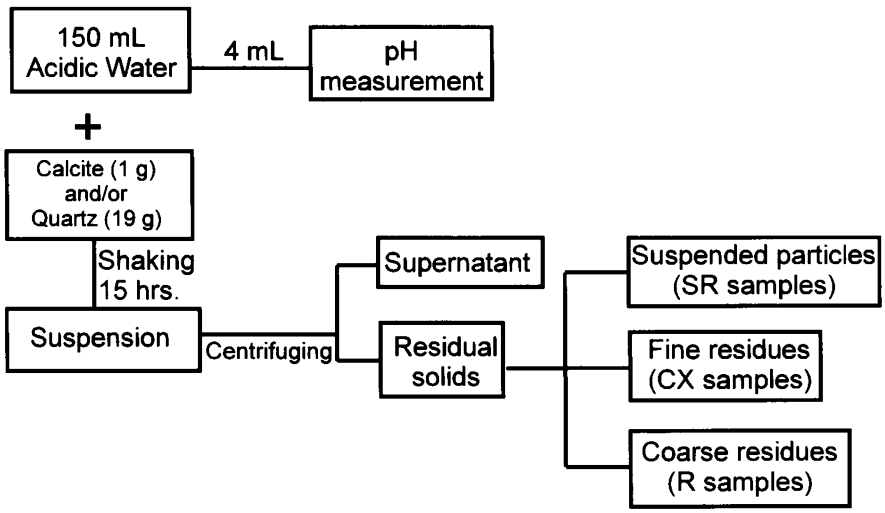

FIG. 1. Schematic diagram showing the experimental procedures used in the study.

Geochemical Modeling

Geochemical modeling of chemical equilibria was conducted with the MINTEQA2 computer code (Allison et al., 1991). The input temperature was 25°C. The measured final pH values and concentrations of various components were used as model input. Quartz and calcite were treated as finite solid phases according to the quantities used. All of the reaction systems werre assumed to be in equilibrium with atmospheric CO_2 ($P_{CO2} = 10^{-3.5}$) based on the experimental method just described. No solid phases were allowed to precipitate in the simulations and the potential for precipitation was evaluated by the saturation index [log(Q/K), Q = reaction quotient, K = equilibrium constant] obtained in the calculations.

RESULTS AND DISCUSSION

Solution Chemistry

The ICP analytical results of final supernatants from all treatments indicate that the concentrations of K, Na, and Mg did not differ significantly from the starting solutions. Therefore, these metals are regarded as conservative species and are, therefore, not discussed. pH values and concentrations of metals are listed in Table 3 for both the original solutions and the final supernatants.

In the experiments where calcite was present (treatments 11–14), solution pH increased dramatically. With Fe present in the original solutions, pH changed from 2.4 to above 6.5 (Table 3). The dissolution of calcite resulted in the increases of pH and Ca concentrations in the final solutions. Aluminum in the solutions was almost completely removed because of $Al(OH)_3$ precipitation at final pHs near 7.0. The X-ray diffraction (XRD) analyses of solid residues from these treatments did not detect any crystalline Al phases. Meng and Letterman (1993) observed amorphous $Al(OH)_3$ coated on silica surfaces under similar experimental conditions. As pH increased, Fe^{3+} was precipitated out as ferrihydrite. XRD analyses of the final solid residues revealed a broad peak centered at 2.5 Å, which corresponds to that of ferrihydrite with poor crystallinity (Bigham et al., 1992; Schwertmann and Taylor, 1989). Loeppert et al. 1994 also found that ferrihydrite was the only solid product in the Fe^{3+}-calcite reaction system. Concentrations of Cu and Pb decreased significantly in these experiments (treatments 11–14), whereas that of Zn and Cd decreased to a lesser extent.

In treatment 11 where no Fe was present in the original solution, the initial pH was 4.24. This value was much higher than any of other treatments (*ca.* 2.4). As a result, less calcite was dissolved in the experiment and the final Ca concentration (150 mg/L) was much lower than that in the other treatments. In treatment 15 where quartz was the only initial solid, the chemistry of final solution was not significantly different from the starting solution except for Fe concentration. Ferrihydrite was identified in the final solid residue by XRD. The precipitation of ferrihydrite resulted in a slight pH decrease from 2.43 to 2.26 during the following reaction:

$$5\ Fe^{3+} + 12\ H_2O = Fe_5HO_8{\cdot}4H_2O + 15\ H^+ \quad (1)$$

Although ferrihydrite precipitation is not common at such a low pH, the precipitation can be accelerated by the high sulfate concentration in the solution even at low pH (Flynn, 1984).

Solid Composition and Morphology

Figure 2 depicts the SEM micrographs of calcite (Fig. 2A) and quartz (Fig. 2B) grains after the reaction in treatment 12. The calcite grain is characterized by ubiquitous

TABLE 3. CHANGES OF SOLUTION CONCENTRATIONS FOR VARIOUS TREATMENTS: ALL CONCENTRATIONS ARE IN MG/L, MEASURED BY FLAME AA EXCEPT AS OTHERWISE INDICATED

Treatment	*Al*[a]	*Ca*	*Zn*	*Cd*	*Pb*	*Cu*	*Fe*	*pH*
11R	27	—	131	5.62	10.4	127	—	4.24
11F	b.d.	150	93.5	5.60	3.71	4.41	—	6.57
12R	27	—	131	5.62	10.4	127	560	2.42
12F	0.03	614	97.2	5.03	0.20	8.7	0.56	6.33
13R	27	—	—	—	—	—	560	2.42
13F	0.07	591	—	—	—	—	1.12	6.97
14R	27	—	131	5.62	10.4	127	560	2.44
14F	0.14	641	93.5	4.86	0.20	6.2	0.79	7.35
15R	27	—	131	5.62	10.4	127	560	2.43
15F	26.9	0.09	115.3	5.54	9.95	125	283	2.26

[a]ICP analyses.

R = original solution, F = final solution after reaction, — = component not present, b.d. = below detection of 0.01 mg/L.

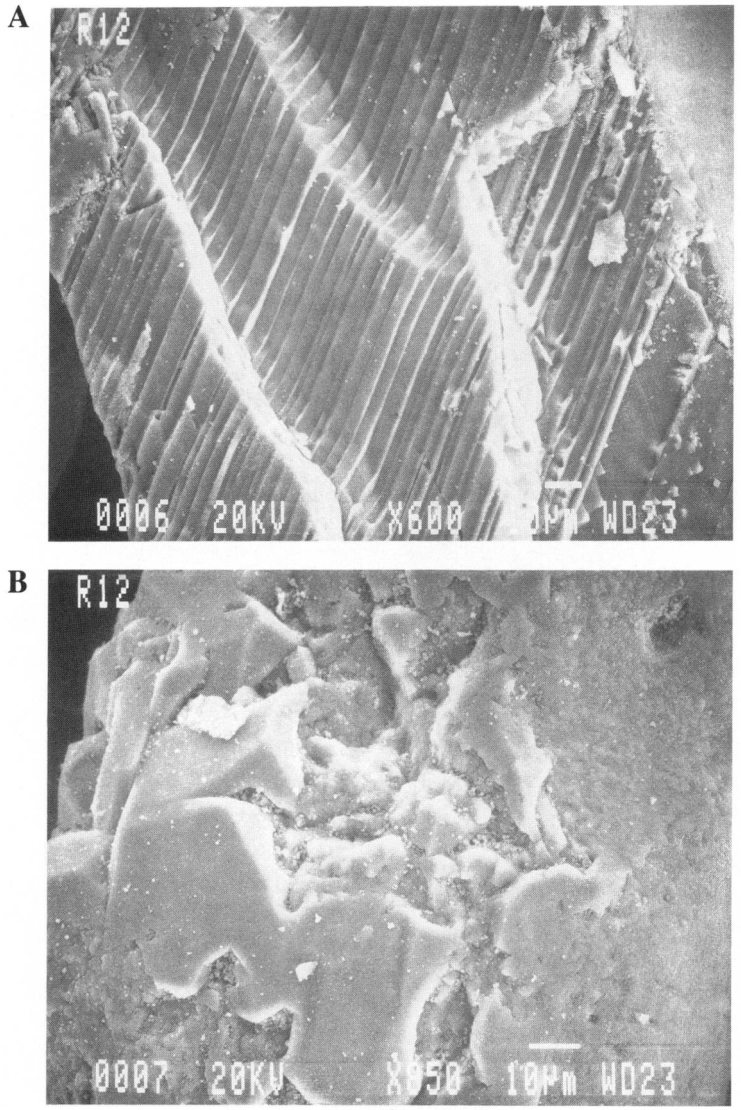

FIG. 2. SEM micrographs of solid residue from treatment 12 (sample R12), showing the surfaces of a calcite grain (A) and a quartz grain (B).

dissolution steps, whereas the quartz grain was coated, presumably with ferrihydrite which was identified by XRD. The coating of ferrihydrite on the quartz surfaces has been observed in laboratory studies (Fryar, 1992; Stollenwerk, 1991). The presence of a ferrihydrite coating on quartz and its absence on calcite can be interpreted with the surface charge characteristics of these solids. The Point of Zero Charge (PZC) of ferrihydrite is in the range of 7.9 to 8.2 (Dzombak and Morel, 1990), whereas PZCs for calcite and quartz are 10.0 and 2.0, respectively (Sposito, 1984). Therefore, ferrihydrite and calcite are positively charged and quartz is negatively charged in the pH range of 2.0 to 8.0, which was the operable range in most of our experiments. As a result of these changed conditions, ferrihydrite tended to precipitate on the quartz surfaces rather than the calcite. The significance of this surface coating is that calcite can provide a continuous source of neutralizing agent to water acidity, whereas quartz surfaces serve as reservoirs for Fe-oxide precipitates. Besides ferrihydrite, $Al(OH)_3$ with PZC = 9.1 (Meng and Letterman, 1993) may also precipitate on quartz surfaces. When a calcareous soil receives acid-mine waters from mining, a similar phenomenon would be expected.

Sorption of ions on Fe and Al hydroxides may be revealed by FTIR spectra. Figure 3 displays a FTIR spectrum of the SR12 in treatment 12. Among the bands assigned in Fig. 3, the peaks at 1100 and 617 cm^{-1} are

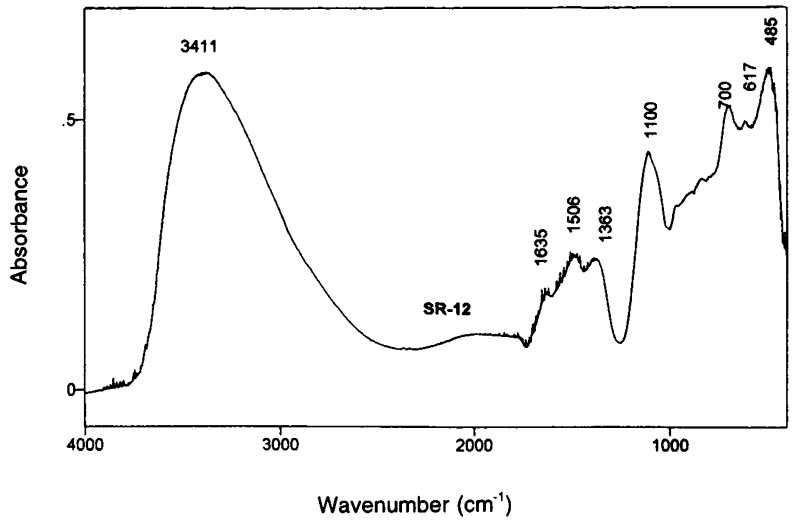

FIG. 3. DR–FTIR spectrum of the solid reaction product from treatment 12 (sample SR12). The absorbance peaks are assigned as OH stretching at 3411 cm^{-1} (Farmer, 1974), OH bending (?) at 1506 and 1363 cm^{-1}, and Fe-O stretching at 700 and 485 cm^{-1} (Bigham et al., 1990). The bands at 1100 and 617 cm^{-1} are assigned as $\nu_3(SO_4)$ and $\nu_4(SO_4)$.

$\nu_3(SO_4)$ and $\nu_4(SO_4)$. They correspond to the fundamental vibration frequencies of SO_4 at T_d symmetry in which only the ν_3 and ν_4 bands are infrared active (Bigham et al., 1992; Farmer, 1974). The T_d symmetry reflects a typical free ion state of SO_4^{2-}. Therefore, sulfate ion was weakly adsorbed (as an outer-sphere complex) on the available solid surfaces.

In a system without quartz (treatment 14), the morphology of ferrihydrite was quite different. SEM micrographs of the solid R14 are illustrated in Fig. 4. In general, ferrihydrite is loosely scattered in the voids among calcite grains (Fig. 4A). A close examination reveals several cases of partial coverage of ferrihydrite on calcite surfaces (Fig. 4B). This partial coverage appears to be a result of physical deposition during the drying of the sample.

When no Fe was present in the original solution (treatment 11), ferrihydrite was absent in the final products. The relatively high solution concentrations of Pb and Cd at the end of treatment 11 appear to have been resulted from reduced adsorption in the absence of ferrihydrite surfaces. An additional crystalline phase was detected in the CX11 sample (Fig. 5). Quartz and calcite were both present along with a new set of diffraction peaks. The most prominent ones were centered at 2.714 Å and 1.50 Å. Figure 6 shows a SEM micrograph of the sample (Fig. 6A), together with an X-Ray EDS focused on a single aggregate of precipitates in the sample (Fig. 6B). The EDS reveals the abundance of Zn, Al, S, and Cu in the aggregate. The Al signal is likely from $Al(OH)_3$. Therefore, the new phase is likely a Zn and/or Cu sulfate. An extensive search based on the XRD pattern leads to two closest matches: $(Cu,Zn)_7(SO_4)_2(OH)_{10}\cdot 3H_2O$ (Schulenbergite) and $(Cu,Zn)_4SO_4(OH)_6\cdot 4H_2O$ (Namuwite).

In the system without calcite (treatment 15), ferrihydrite precipitation occurred but to much less extent than with the other systems just described. Besides the ferrihydrite, the XRD pattern for the solid residue (sample CX15) also revealed both peaks of 2.714 Å and 1.50 Å that are found in Fig. 5. Figure 7 includes a SEM micrograph of sample CX15 (Fig. 7A) and an EDS spectrum focused on the cluster of precipitates on the surface of the sample (Fig. 7B). Based on the aforementioned discussion, the precipitates consisted mainly of ferrihydrite, $Al(OH)_3$ and the new sulfate phase. The EDS spectrum in Fig. 7B detects Fe, S, and Al in the precipitates. The finding is consistent with the XRD and chemical results presented earlier. The presence of the sulfate phase is further supported by the FTIR spectrum of the solid residue (sample SR15) depicted in Fig. 8. In comparison with the spectrum in Fig. 3 (treatment 12), the extra OH stretching bands at 3694, 3654, and 3619 cm^{-1} reveal the presence of structural H_2O (Farmer, 1974). The $\nu_3(SO_4)$ previously centered at 1100 cm^{-1} is now split into several peaks (1102, 1038 cm^{-1}, and others), indicating much lower SO_4 site symmetry (e.g., C_1 symmetry). SO_4 resides in a crystal structure in this symmetry. The $\nu_1(SO_4)$ and $\nu_2(SO_4)$ bands become infrared active and they are assigned as 980 and 529 cm^{-1}, respectively. These observations further confirm that the novel phase is a sulfate with structural H_2O.

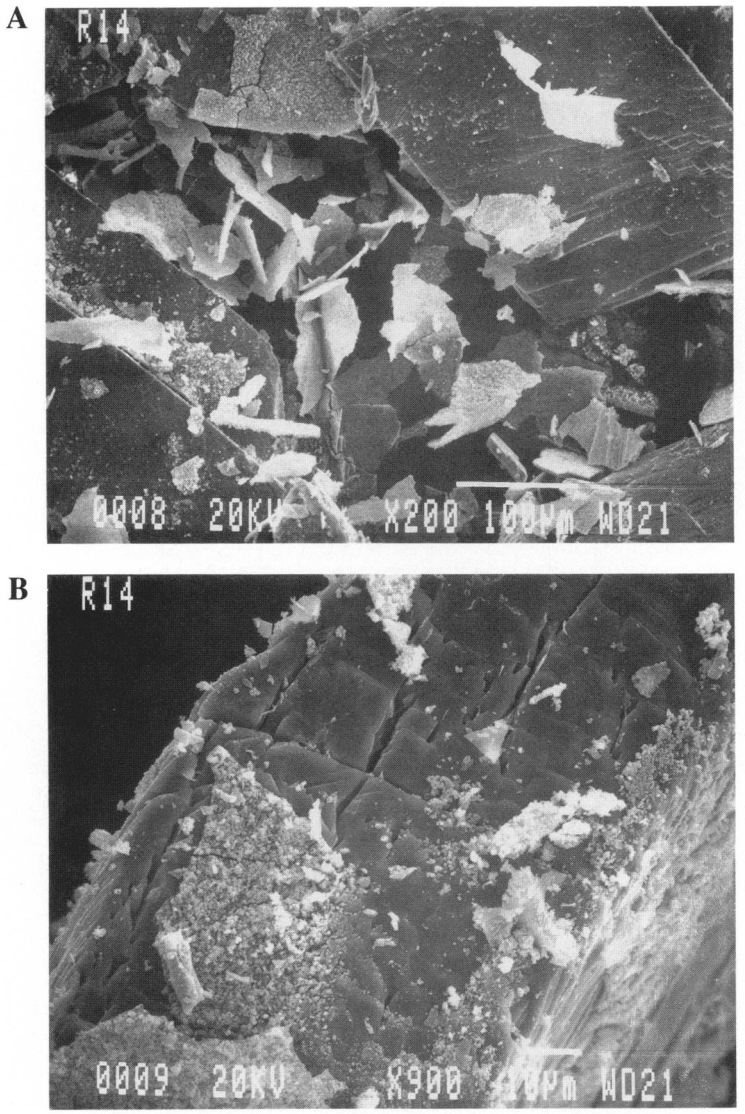

FIG. 4. SEM micrographs of solid residue from treatment 14 (sample R14). (A) Clusters of precipitates scattering around the larger calcite grains and (B) a close-up view of a cluster on the surface of a calcite grain.

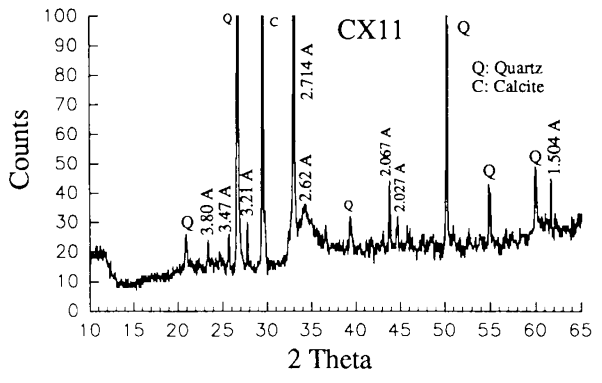

FIG. 5. X-Ray Diffraction (XRD) pattern of solid residue from treatment 11 (sample CX11).

Metal Distribution

The important processes regulating metal mobility in the systems studied were precipitation and adsorption. Besides $Al(OH)_3$ and ferrihydrite, $Cu(OH)_2$ was likely present in some of the experimental treatments based on its saturation index from MINTEQA2 calculations. Sorption of metal ions to various solid surfaces becomes very important when precipitates such as ferrihydrite and $Al(OH)_3$ occur. Because of large surface areas of these precipitates, they provide extensive surface sites for sorption. However, these sites are often selective to metal ions and adsorption is often pH dependent. In a multi-ion system like the one in this study, competition among the ions for the surface sites becomes important.

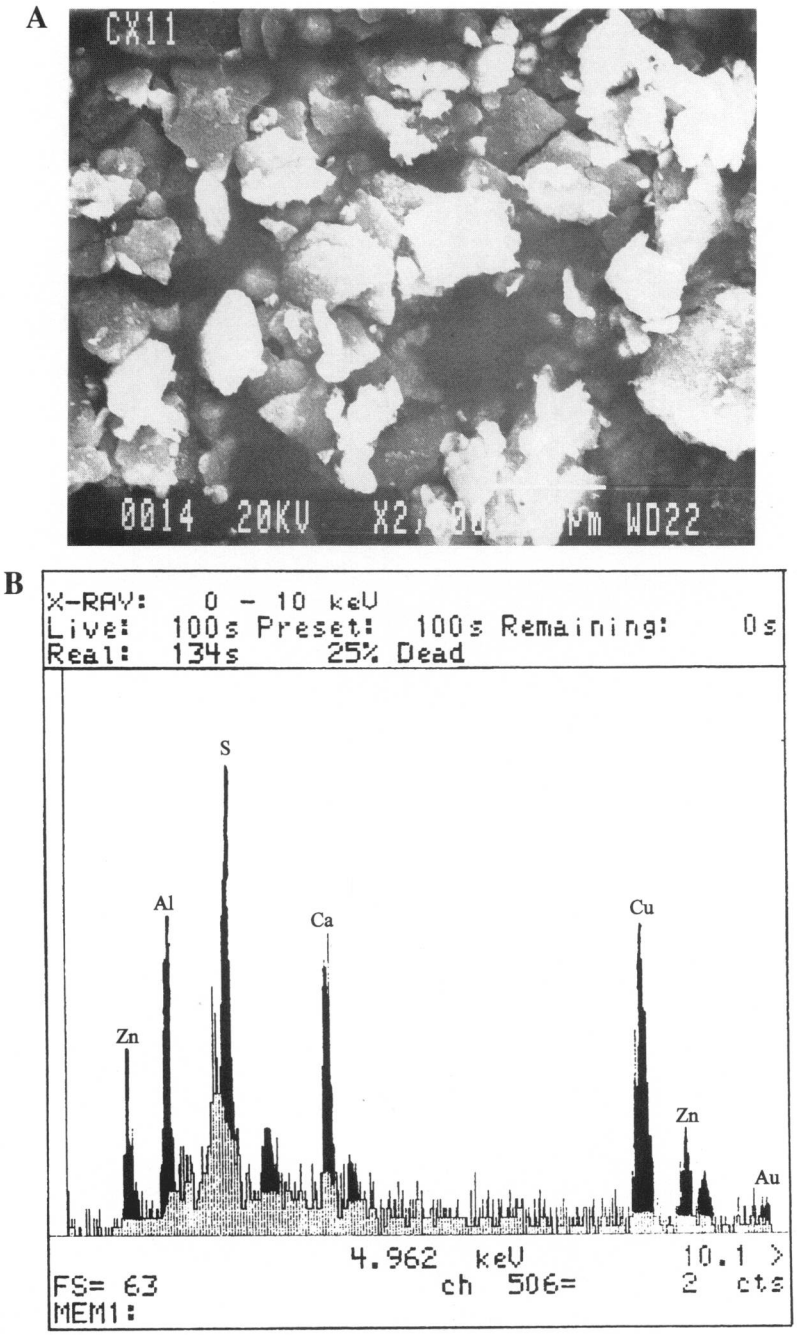

FIG. 6. Electron microscopic examination of solid residue from treatment 11 (sample CX11). (A) SEM micrograph showing clusters of precipitates and (B) X-Ray EDS of precipitates.

The experimental results from this study showed that Pb and Cu are more easily retained than Cd and Zn. The results are consistent with that observed by Kinniburgh et al. (1976) for iron and aluminum oxides. The removal of Pb from the solution can be attributed to several possibilities. Pb^{2+} adsorb significantly on the surfaces of quartz, $Al(OH)_3$ and calcite through a variety of surface reactions (Sposito, 1984). The presence of ferrihydrite promotes strong adsorption of Pb^{2+}. Müller and Sigg 1992 estimated that Pb^{2+} adsorption capacity on the goethite they used was 3.8×10^{-6} mol/m^2. With the larger specific surface area of ferrihydrite, larger adsorption capacity is expected.

Cd removal can be explained by Cd sorption to the

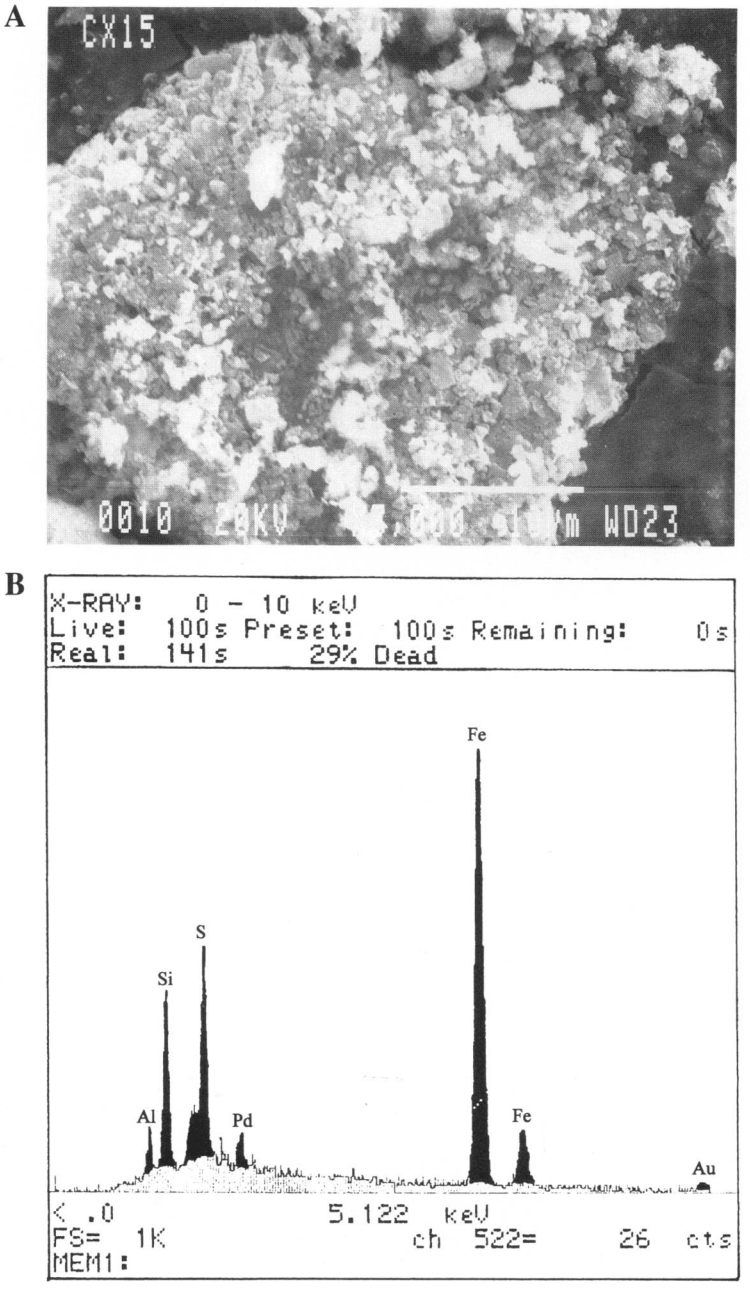

FIG. 7. Electron microscopic examination of solid residue from tratment 15 (sample CX15). (A) SEM micrograph showing clusters of precipitates on quartz surfaces and (B) EDS focused on the cluster of precipitates shown in (A).

surfaces of quartz (Liu et al., 1993) calcite (McBridge, 1980; Stipp et al., 1992; Davis et al., 1987), amorphous $Al(OH)_3$ and ferrihydrite. A comparison of the results between treatment 11 and the other treatments in Table 2 indicates that the ferrihydrite surface is likely to have provided the majority of sorption sites for aqueous Cd. Cowan et al. (1991) and other investigators showed that Cd^{2+} adsorption on amorphous Fe oxide occurred between pH 5.5 and 8.5 and that 50% of the total Cd was sorbed at pH values of 6.4 and 6.7 for Cd initial concentrations of 10^{-7} and 10^{-6} M, respectively. Meng and Letterman (1993) observed a similar pH range at a higher Cd^{2+} concentration (1.78×10^{-5} M) with 50% adsorption evident at about pH 6.5. The results of an additional run that was identical to treatment 12 but without Pb, Zn, and Cu showed that about 50% Cd adsorption at $[Cd]_T = 5 \times 10^{-5}$ M was achieved with the mixed solids of ferrihydrite, $Al(OH)_3$, calcite and quartz at pH 6.86. The ex-

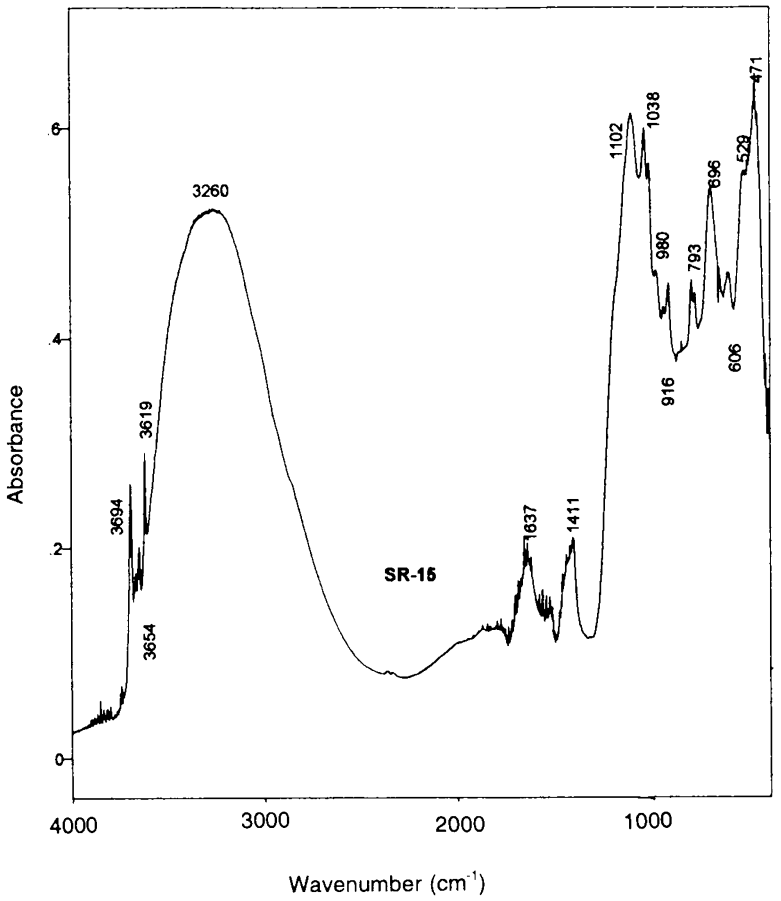

FIG. 8. FTIR spectrum of solid residue from treatment 15 (sample SR15). In addition to the peaks assigned in Fig. 3, the extra OH stretching bands at 3694, 3654, and 3619 cm^{-1} indicate the presence of structural H_2O [26]. The $\nu_3(SO_4)$ previously centered at 1100 cm^{-1} is split into several peaks (1102, 1038 cm^{-1}, and others). The 980 and 529 cm^{-1} peaks are assigned as $\nu_1(SO_4)$ and $\nu_2(SO_4)$, respectively.

tent of adsorption is comparable to that of Meng and Letterman (1993). In treatments 12 and 14, however, Cd removal rates were much less than 50%, likely due to competition among the metal ions. The competition of Ca^{2+} and Cd^{2+} for the oxide surface can also cause less Cd adsorption (Cowan et al., 1991; Petersen et al., 1993).

The removal of Zn from the solution appears to be associated with precipitation of $Zn(OH)_2$ and the new sulfate phase at the high initial Zn concentrations (Lindsay, 1979). Other factors contributing to the removal include Zn sorption to quartz (Liu et al., 1993), calcite (Zachara et al., 1988; 1989; 1991) and the amorphous $Al(OH)_3$ precipitate.

Ionic complexation influence the adsorption as well. For example, the formation of $CdSO_4^0$ can weaken the Cd sorption to iron oxide surfaces (Benjamin and Leckie, 1982). This speciation effect becomes more sigificant in higher ionic strength solutions and effectively reduces Cd^{2+} activity. The high ionic strength and sulfate concentration in our system promoted the formation of $CdSO_4^0$ species which is supported by a MINTEQA2 simulation. Similar complexation effect has been reported for Zn sorption (Benjamin and Leckie, 1982).

ACKNOWLEDGMENTS

We thank Jerry Bigham for his assistance in XRD analyses. Satish Mynemi is acknowledged for his valuable contribution to the interpretation of FTIR spectra. Partial support was provided through Ohio Eminent Scholar fund to FWS and The Ohio State University Presidential Fellowship to the senior author.

REFERENCES

ALLISON, J.D., BROWN, D.S., and NOVO-GRADAC, K.J. (1991). MINTEQA2/PRODEFA2, a geochemical assessment model for environmental systems: Version 3.0 user's manual. U.S. Environmental Protection Agency, Athens, GA, EPA/600/3–91/021.

BATES, M.H., VEENSTRA, J.N., BARBER, J., BERNARD, R., KARLESKINT, J., KHAN, P., PAKANTI, R., and TATE, M. (1990). Physical-chemical treatment of acid mine water from a Superfund site. *J. Environmental Systems,* **19,** 237–263.

BENJAMIN, M.M., and LECKIE, J.O. (1982). Effects of complexation by Cl, SO_4, and S_2O_3 on adsorption of Cd on oxide surfaces. *Environ. Sci. Technol.* **16,** 162–170.

BIGHAM, J.M., SCHWERTMANN, U., and CARLSON, L. (1992). Mineralogy of precipitates formed by the biogeochemical oxidation of Fe(II) in mine drainage in *Biomineralization, Processes of Iron and Manganese,* H.C.W. Skinner and R.W. Fitzpatrick, Eds. Caterna Supplement 21, International Society of Soil Science.

BIGHAM, J.M., SCHWERTMANN, U., CARLSON, L., and MURAD, E. (1990). A poorly crystallized oxyhydroxysulfate of iron formed by bacterial oxidation of Fe(II) in acid mine waters. *Geochim. Cosmochim. Acta,* **54,** 2743–2758.

BOLING, S.D., KOBYLINSKI, E.A., and MICHAEL, J.I. (1992). Process removes metals from acid mine drainage. *Water Environment & Technology,* **4,** 26–27.

CHIRONIS, N.P. (1992). Mine-build ponds economically clear acid mine waters. *Coal Age,* **92,** 58–61.

COWAN, C.E., ZACHARA, J.M., and RESCH, C.T. (1991). Cadmium adsorption on iron oxides in the presence of alkaline-earth elements. *Environ. Sci. Technol.* **25,** 437–446.

DAVIS, J.A., FULLER, C.C., and COOK, A.D. (1987). A model for trace metal sorption processes at the calcite surface: Adsorption of CD^{2+} and subsequent solid solution formation. *Geochim. Cosmochim. Acta* **51,** 1477–1490.

DZOMBAK, D.A., and MOREL, F.M.M. (1990). Surface complexation modeling. Wiley-Interscience, New York.

FARMER, V.C. (1974). The infrared spectra of minerals. Mineralogical Society Monograph 4, Mineralogical Society, London.

FAURE, G. (1991). *Principles and applications of inorganic geochesmistry.* MacMillan, New York, p. 313.

FILIPEK, L.H., NORDSTROM, D.K., and FICKLIN, W.H. (1987). Interaction of acid mine drainage with waters and sediments of West Squaw Creek in the West Shasta Mining District, California. *Environ. Sci. Technol.* **21,** 388–396.

FLYNN, C.M., Jr. (1994). Hydrolysis of inorganic iron (III) salts. *Chem. Rev.* **84,** 31–41.

FRYAR, A.E. (1992). The geochemical and hydraulic evolution of reaction fronts in sand columns. Unpublished Ph.D. thesis, University of Alberta, Edmonton, Alberta, Canada.

HAMMEN, R.F., PANG, D.C., VAN DER SLUYS, L.S., JUDD, R.C., and LOFTSGAARDEN, E. (1993). Acid mine water processing and metal recovery by fast solid phase extraction. *Mining Engineering,* **45,** 58–61.

HEUNISCH, G.W. (1987). Lime substitutes for the treatment of acid mine drainage. *Mining Engineering,* **39,** 33–36.

JENKE, D.R., and DIEBOLD, F.E. (1984). Electroprecipitation treatment of acid mine wastewater. *Water Res.* **18,** 855–859.

KINNIBURGH, D.G., JACKSON, M.L., and SYERS, J.K. (1976). Adsorption of alkaline earth, transition, and heavy metal cations by hydrous oxide gels of iron and aluminum. *Soil Sci. Soc. Am. J.* **40,** 796–799.

LINDSAY, W.L. (1979). *Chemical equilibria in soils.* Wiley-Interscience, New York.

LIU, J., HOWARD, S.M., and HAN, K.N. (1993). Adsorption behavior of cadmium and zinc ions on oxide/water interfaces. *Langmuir,* **9,** 3635–3639.

LOEPPERT, R.H., HOSSNER, L.R., and AMIN, P.K. (1984). Formation of ferric oxyhydroxides from ferrous and ferric perchlorate in stirred calcareous systems. *Soil Sci. Soc. Am. J.* **48,** 677–683.

MACHEMER, S.D., and WILDEMAN, T.R. (1992). Adsorption compared with sulfide precipitation as metal removal processes from acid mine drainage in a constructed wetland. *J. Con-taminant Hydrology,* **9,** 115–131.

McBRIDE, M.B. (1980). Chemisorption of Cd^{2+} on calcite surfaces. *Soil Sci. Soc. Am. J.* **44,** 26–28.

MENG, X., and LETTERMAN, R.D. (1993). Effect of component oxide interaction on the adsorption properties of mixed oxides. *Environ. Sci. Technol.* **27,** 970–975.

MERRILL, D.T., MANZIONE, M.A., PETERSON, J.J., PARKER, D.W., CHOW, W., and HOBBS, A.O. (1986). Field evaluation of arsenic and selenium removal by iron coprecipitation. *Journal WPCF,* **58,** 18.

MÜLLER, B., and SIGG, L. (1992). Adsorption of lead(II) on the goethite surface: Voltammetric evaluation of surface complexation parameters. *J. Colloid Interface Sci.* **148,** 517–532.

OMURA, T., UMITA, T., NENOV, V., ZIZAWA, J., and ONUMA, M. (1991). Biological oxidation of ferrous iron in high acid mine drainage by fluidized bed reactor. *Wat. Sci. Tech.* **23,** 1447–1456.

PETERSEN, W., WALLMANN, K., and SCHROEDER, F. (1993). Studies on the adsorption of cadmium on hydrous iron(III) oxides in oxic sediments. *Analytica Chimica Acta,* **273,** 323–327.

SASOWSKY, I.D., and WHITE, W.B. (1993). Geochemistry of the Obey River Basin, north-central Tennessee: A case of acid mine water in a karst drainage system. *J. Hydrology,* **146,** 29–48.

SCHWERTMANN, U., and TAYLOR, R.M. (1989). Iron oxides. In *Minerals in Soil Environments, 2nd ed.,* Dixon, J.B., and Weed, S.B., Eds., Soil Science Society of America, Madison, WI, pp. 379–438.

SPOSITO, G. (1984). *Surface chemistry of soils.* Oxford Univ. Press, New York.

STIPP, S.L., HOCHELLA, Jr., M.F., PARKS, G.A., and

LECKIE, J.O. (1992). Cd^{2+} uptake by calcite, solid-state diffusion, and the formation of solid-solution: Interface process observed with near-surface sensitive techniques (XPS, LEED, and AES). *Geochim. Cosmochim. Acta,* **56,** 1941–1954.

STOLLENWERK, K.G. (1991). Stimulation of molybdate sorption with the diffuse layer surface–complexation model. In *U.S. Geological Survey Toxic Substance Hydrology Program—Proceedings of the Technical Meeting, Monterey, CA,* March 11–15, Mallard, G.E., and Aronson, D.A., Eds., Water Resources Investigation Report 91–4034, pp. 47–52.

WINLAND, R.L. (1989). Acid coal mine drainage in Ohio: Stream water quality, precipitate chemistry and mineralogy. Unpublished MS. thesis, Ohio State University.

WINLAND, R.L., TRAINA, S.J., and BIGHAM, J.M. (1991). Chemical composition of ochreous precipitates form Ohio coal mine drainage. *J. Environ. Qual.* **20,** 452–460.

ZACHARA, J.M., COWAN, C.E., and RESCH, C.T. (1991). Sorption of divalent metals on calcite. *Geochim. Cosmochim. Acta,* **55,** 1549–1562.

ZACHARA, J.M., KITTRICK, J.A., DAKE, L.S., and HARSH, J.B. (1989). Solubility and surface spectroscopy of zinc precipitates on calcite. *Geochim. Cosmochim. Acta,* **53,** 9–19.

ZACHARA, J.M., KITTRICK, J.A., and HARSH, J.B. (1988). The mechanism of Zn^{2+} adsorption on calcite. *Geochim. Cosmochim. Acta,* **52,** 2281–2291.

Address correspondence to:
Charlie Y. Xu
Dept. 26
Chemical Abstracts Service
2540 Olentangy River Rd.
Columbus, OH 43210
e-mail: cxu@cas.org